Appl Biochem Biotechnol (2008) 150:243–257
DOI 10.1007/s12010-007-8127-6

Non-Selective Toxicological Effects of the Insect Juvenile Hormone Analogue Methoprene. A Membrane Biophysical Approach

João P. Monteiro · Romeu A. Videira · Manuel J. Matos · Augusto M. Dinis · Amália S. Jurado

Received: 13 September 2007 / Accepted: 7 December 2007 /
Published online: 31 January 2008

Abstract The Gram-positive bacterium, *Bacillus stearothermophilus*, was used as a model organism to identify the non-selective toxic effects of the currently used insecticide methoprene (isopropyl(2E,4E)-11-methoxy-3,7,11-trimethyl-2,4-dodecadienoate). A significant decrease of the yield of bacterial cultures and a premature appearance of ultrastructural abnormalities in cells cultured in the presence of the insecticide were taken as indicators of cytotoxicity. A putative correlation of this cytotoxicity with methoprene-induced perturbations on membrane lipid organization was investigated, using differential scanning calorimetry and the fluorescence polarization of 1,6-diphenyl-1,3,5-hexatriene (DPH) and its propionic acid derivative (DPH–PA). The membrane physical effects depended on the lipid bilayer composition and packing. The most striking effect was a progressive broadening and shifting to lower temperatures, with increasing methoprene concentrations, of the main transition phase of the dimyristoyl- or dipalmitoylphosphatidylcholine bilayers and of the lateral phase separation of liposomes reconstituted with the lipid extracts of *B. stearothermophilus.*

Keywords Methoprene · Lipid dynamics · Differential scanning calorimetry · Fluorescence polarization · Cell ultrastructure · *Bacillus stearothermophilus*

J. P. Monteiro · M. J. Matos · A. S. Jurado
Centro de Neurociências e Biologia Celular; Department of Biochemistry, University of Coimbra, 3001-401 Coimbra, Portugal

R. A. Videira
Higher School of Technology, Polytechnic Institute of Viseu, 3504-510 Viseu, Portugal

A. M. Dinis
Laboratório de Microscopia Electrónica, Department of Botany, University of Coimbra, 3001-401 Coimbra, Portugal

A. S. Jurado (✉)
Department of Biochemistry, University of Coimbra, Apartado 3126, 3001-401 Coimbra, Portugal
e-mail: asjurado@ci.uc.pt

Abbreviations

DMPC	dimyristoylphosphatidylcholine
DPH	1,6-diphenyl-1,3,5-hexatriene
DPH-PA	3-(*p*-(6-phenyl)-1,3,5-hexatrienyl)phenylpropionic acid
DPPC	dipalmitoylphosphatidylcholine
DSC	differential scanning calorimetry
TEM	transmission electron microscopy

Introduction

Methoprene (Fig. 1) is an insecticide of general use that mimics the action of an insect growth regulation hormone, thus, interfering with the insect normal maturation process. Accordingly, methoprene prevents recurring infestation, artificially stunting the insects' development by breaking their life cycle and making it impossible for them to mature to the adult stages [1]. However, deleterious effects of methoprene have been reported for a variety of other organisms, like crustaceans [2, 3] and fishes [4, 5]. In the late 1990s, a possible relationship of methoprene with the increase of malformed amphibians in North America [6, 7] triggered a considerable amount of toxicity research to assess more accurately the risk of this insecticide for non-target species. Although it has been recently suggested that methoprene by itself could not originate amphibian malformations [8], the molecular mechanisms underlying the toxicity of the compound for non-target organisms are far from being clear.

Because of the lipophilic character of the methoprene molecule [9], its incorporation into biomembranes is predictable. The effects of lipophilic molecules on the physico-chemical properties of lipid membranes have drawn a considerable attention from a toxicological point of view [10]. A growing body of evidence has shown the influence of the structure and dynamics of the lipid bilayer in the membrane/cell functionality [10, 11]. In addition, biomembranes are common components to all living systems and, therefore, are good candidates as a biological target involved in xenobiotics' unselective toxic effects.

Bacillus stearothermophilus has been used as a tool model to study the toxicity of lipophilic xenobiotics at the cell level because the growth and morphology of this bacterium is strongly affected by environmental agents (drugs, ions, and temperature) that induce alterations on the physical properties of membrane lipids [12–15].

Following previous research [16], the present work aims to further elucidate the possible relationship between the membrane physical effects and the methoprene toxicity. As a starting step toward understanding methoprene–biomembrane interactions, model membranes of synthetic phosphatidylcholines of different acyl chains length (DMPC or DPPC) were used to investigate the pesticide effects on the physical properties of a simple lipid bilayer. To obtain more realistic membrane models, liposomes consisting of the lipids extracted from *B. stearothermophilus* membranes were prepared [13]. This combined approach allows us to gain insight of the way methoprene interacts with the lipid bilayer. The experimental data reported in the present work may be helpful to further clarify the influence of membrane biophysical alterations on the cytotoxic effects of lipophilic xenobiotics, in general, and of methoprene, in particular.

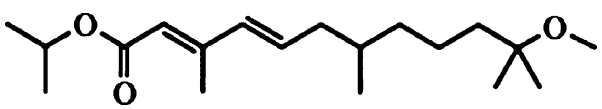

Fig. 1 Molecular structure of methoprene

Materials and Methods

Chemicals

The lipids dimyristoyl- and dipalmitoylphosphatidylcholine (at least 98% pure) and the insecticide methoprene (94.9% purity) were obtained from Sigma Chemical Co. (St. Louis, MO, USA). The probes 1,6-diphenyl-1,3,5-hexatriene (DPH) and 3-(*p*-(6-phenyl)-1,3,5-hexatrienyl) phenylpropionic acid (DPH-PA) were purchased from Molecular Probes, Inc. (Eugene, OR, USA). All the other chemicals were of the highest commercially available purity.

Bacterial Cultures

The strain of *B. stearothermophilus* and the conditions for its maintenance and growth have been described elsewhere [13]. Liquid cultures started with an early stationary inoculum were grown in 1 l Erlenmeyer flasks containing 200 ml of diluted L-broth (Luria broth), shaken at 130 strokes/min in a New Brunswick water bath shaker at 65 °C. Cultures with methoprene were grown in diluted L-broth to which aliquots of a concentrated ethanolic solution of methoprene were added to obtain concentrations ranging from 7.5 to 25 μM. Controls were grown in a medium without insecticide, containing a few microliters of ethanol corresponding to the maximal volume of the methoprene solution assayed. Growth was monitored by measuring the turbidity at 610 nm in a Bausch & Lomb Spectronic 21 spectrophotometer.

Transmission Electron Microscopy

Two milliliters of 25% glutaraldehyde were added to aliquots (20 ml) of the different cultures (with and without 20-μM methoprene) harvested at specific times. After centrifugation at 4000×*g* for 5 min, the pellets were resuspended in 2.5% glutaraldehyde in 0.1 M cacodylate buffer, pH 7.2, supplemented with 0.1 M $CaCl_2$, and left for 2 h at 4 °C. Then, the cells were washed with the same buffer and postfixed at room temperature for 1.5 h in 1% buffered osmium tetroxide. After post-staining with 1% aqueous uranyl acetate for 1 h in the dark at room temperature, the cells were dehydrated in a graded ethanol series (70–100%) and embedded in low-viscosity resin [17]. Previous to dehydration, the cells were concentrated and pre-embedded by centrifugation in 1.5% agar. Ultrathin sections were obtained with an ultramicrotome LKB Ultrotome NOVA equipped with a diamond knife and conventionally stained with lead citrate. Observations were made in a JEOL JEM-100 SX at 80 kV.

The number of normal and abnormal cells contained in the ultrathin sections obtained from two different blocks belonging to the same sample (control 60 min, control 120 min, and methoprene 120 min) was directly counted in the whole fluorescent screen using a magnification of ×15,000. Five to seven count areas were randomly selected in each grid, the total number of cells counted being 425 to 455 for each sample. The number of normal and abnormal cells in each sample was then compared statistically.

Extraction and Analysis of Bacterial Lipids

Cells grown up to the beginning of the stationary phase were harvested by low-speed centrifugation and washed three times with buffer (10 mM Tris–Cl, pH 7.0). Lipids were extracted by the method of Bligh and Dyer [18] and quantified by measuring the amount of inorganic phosphate [19], after hydrolysis of the extracts in 70% $HClO_4$ at 180 °C for 60

min [20]. Polar lipids were isolated from the total lipid extract by preparative thin-layer chromatography and extracted as previously described [13]. The lipid extracts (total lipid extract and polar lipid fraction) dissolved in chloroform were stored under nitrogen atmosphere at −20 °C.

Preparation of Liposomes for Fluorescence Polarization and DSC Studies

Aliquots from lipid solutions in $CHCl_3$ (bacterial lipid extracts or the synthetic phosphatidylcholines DMPC and DPPC), containing 10 mg (for DSC) or 2.3 mg of phospholipid (for fluorescence polarization experiments), were evaporated to dryness in a rotary evaporator. The dry residues were hydrated under N_2 atmosphere by gentle shaking with 2–5 ml of 50 mM KCl and 10 mM Tris–maleate (pH 7.0) in a water bath 7–10 °C above the transition temperature of the phospholipids or, for bacterial lipid mixtures, at 65 °C, i.e., a temperature above the lateral phase separation range. Then, the suspensions of multilamellar vesicles were vortexed for 1 min to disperse aggregates and let to stabilize overnight. The phosphatidylcholine membrane preparations used for fluorescence polarization were also briefly sonicated in a low-energy water sonifier for a few seconds to decrease the scattered light. For DSC experiments, liposome suspensions were centrifuged for 45 min at 45,000×*g*, and the wet pellets were used.

Incorporation of Probes and the Insecticide Into Liposomes

A few microliters of DPH and DPH–PA in dimethylformamide were injected into liposome suspensions (345 μM in phospholipid) to give a lipid/probe molar ratio of 300. After incubation overnight in the dark, methoprene was added from a concentrated ethanolic solution. The mixtures were allowed to equilibrate for 30 min at the phase transition temperature of DMPC/DPPC or at 37 °C in the case of the polar lipid extract of the bacterium, as these temperatures favor the incorporation of most insecticides [21, 22]. Control samples were prepared with equivalent volumes of dimethylformamide and ethanol.

DSC Scans

Multilamellar vesicles were prepared (1.5–2.0 mM in phospholipid), and the methoprene was added as described above to obtain the insecticide/lipid molar ratios of 1:6 and 1:12. Controls were obtained adding a few microliters of ethanol corresponding to the maximal volume of the methoprene solution assayed. After 30 min of incubation in the conditions described in "Preparation of Liposomes for Fluorescence Polarization and DSC Studies," the mixtures (lipid plus insecticide or lipid plus ethanol) were centrifuged as described above ("Preparation of Liposomes for Fluorescence Polarization and DSC Studies"). Lipid pellets were sealed into aluminum pans, and heating scans were performed over an appropriate temperature range on a Perkin–Elmer Pyris 1 differential scanning calorimeter at a scan rate of 5 °C/min. To check the reproducibility of data, three heating scans were recorded for each sample. To compensate the effect of the high heat capacity of the aqueous medium on the baseline, an estimated amount of buffer in the sample was used in the reference pan. Data acquisition and analysis were performed using the software provided by Perkin–Elmer. Two distinct temperatures were automatically defined in the thermotropic profiles: the temperature of the onset (T_0) and the temperature at the endotherm peak (T_m). To define the range of the phase transition or lateral phase separation ($T_f - T_o$), a third temperature was determined (T_f) by extrapolating to the baseline a tangent to the

descendent slope of the endothermic peak. These critical transition temperatures were estimated as the mean value of three heating scans on, at least, three different samples from the same preparation. To determine the total amount of phospholipid contained in a pan, the pan was carefully opened at the end of the experiment, the lipid was dissolved with chloroform/methanol (1:1), and the phosphorous content determined using the methodology described above ("Extraction and Analysis of Bacterial Lipids"). The enthalpy (ΔH) values obtained were normalized to the exact phospholipid content in each pan.

Fluorescence Polarization Measurements

The fluorimetric measurements were performed with a Perkin–Elmer spectrofluorimeter, model MPF-66, with a thermostated cell holder. The excitation was set at 336 nm and the emission at 450 nm (5 and 6 nm band pass). The degree of fluorescence polarization (P) was calculated according to Shinitzky and Barenholz [23] from the equation:

$$P = \frac{I_{\parallel} - I_{\perp} G}{I_{\parallel} + I_{\perp} G}$$

where $I_{\parallel}$ and $I_{\perp}$ are the intensities of the light emitted with its polarization plane parallel ($_{\parallel}$) and perpendicular ($\perp$) to that of the exciting beam. G is the grating correction factor for the optical system, given by the ratio of the vertically to the horizontally polarized emission components when the excitation light is polarized in the horizontal plane. All fluorescence measurements were corrected for the contribution of light scattering by using appropriate blanks without added fluorescent probes.

The degree of fluorescence polarization of DPH and DPH–PA reflects rotational diffusion of the probes and, therefore, reports the structural order or membrane fluidity in the bilayer lipid environments where the probes are embedded. Thus, the term fluidity is used in this paper as being inversely proportional to the degree of fluorescence polarization of DPH and DPH–PA probes, and it essentially reflects the rate and the range of motion of phospholipid acyl chains [24].

Statistical Analysis of Data

The results of DSC and fluorescence polarization, i.e., the transition temperature midpoints (T_m), transition temperature ranges ($T_f - T_o$) and enthalpy changes (ΔH) are presented as means ± standard deviation of three to four independent experiments. Multiple comparisons are performed using one-way analysis of variance (ANOVA) with the Student–Newman–Keuls as a post-test. $P<0.05$ was considered significant. This statistical analysis was also applied to the cells counts in the TEM.

Results

Methoprene Effects on Growth and Ultrastructure of *B. Stearothermophilus*

To investigate the toxicological effects of methoprene, the eubacterium *B. stearothermophilus* was used as a model system. The yield of bacterial cultures in L-broth medium doped with the insecticide, as compared with control cultures, was used as a cytotoxicity indicator

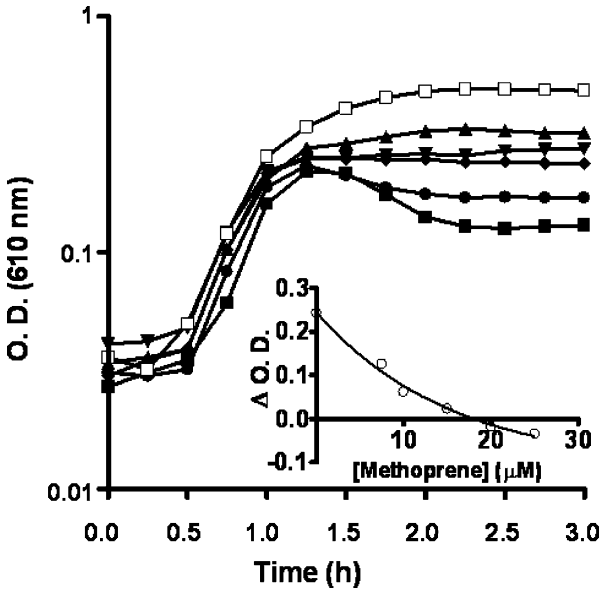

Fig. 2 Effect of methoprene addition on growth of cultures of *B. stearothermophilus* in a basal medium (L-broth) at 65 °C. Cells were grown in the basal medium till the latter exponential phase of growth (60 min of incubation); thereafter, 7.5 (*triangle*), 10 (*inverted triangle*), 15 (*diamond*), 20 (*circle*), and 25 μM (*filled square*) methoprene or a few microliters of ethanol, corresponding to the maximal volume of the methoprene solution assayed (*open square*), were added to the cultures (*arrow*). Growth was measured as optical density (OD) at 610 nm. The results shown are typical of three independent experiences. The *inset* shows the alteration of OD in the period of time between the addition of methoprene (or ethanol, in the case of the control) and 75 min after, as a function of methoprene concentration

(Fig. 2). In parallel, morphological characterization of cells under the influence of the insecticide was performed using the electron microscope (Fig. 3 and Table 1).

After a lag period of approximately 30 min, cultures of *B. stearothermophilus* enter in the exponential phase of growth with a population doubling time of 15 min (Fig. 2). At the end of 1 h of incubation, aliquots of a solution of methoprene in ethanol were injected in the bacterial cultures to obtain a concentration range of 7.5 to 25 μM. In the control culture, a few microliters of pure ethanol, corresponding to the higher volume of methoprene assayed, was added. Thereafter, all the cultures showed a transition stage (retardation phase) linking the logarithmic phase to the stationary phase. Increasing concentrations of methoprene induced a progressive shortening of the retardation phase, during which a factual increase of bacterial population occurred. Simultaneously, the maximal cell yield (maximum population) attained in the stationary phase decreased (Fig. 2). The inset allows to better recognize the alterations promoted by the increasing concentrations of methoprene in the development of the bacterial cultures. Whereas the control culture showed a significant increase of the bacterial population during the 75 min subsequent to the entry in the retardation phase, methoprene-containing cultures showed either a slight increase of cell density followed by an abrupt arrest of growth or, for the highest insecticide concentrations (20 and 25 μM), a rapid transition for a death phase with cell lysis. This was reflected by the decrease in the optical density.

To identify putative cell structural alterations induced by methoprene, aliquots from the control culture and the culture at which 20 μM methoprene was added (Fig. 2) were

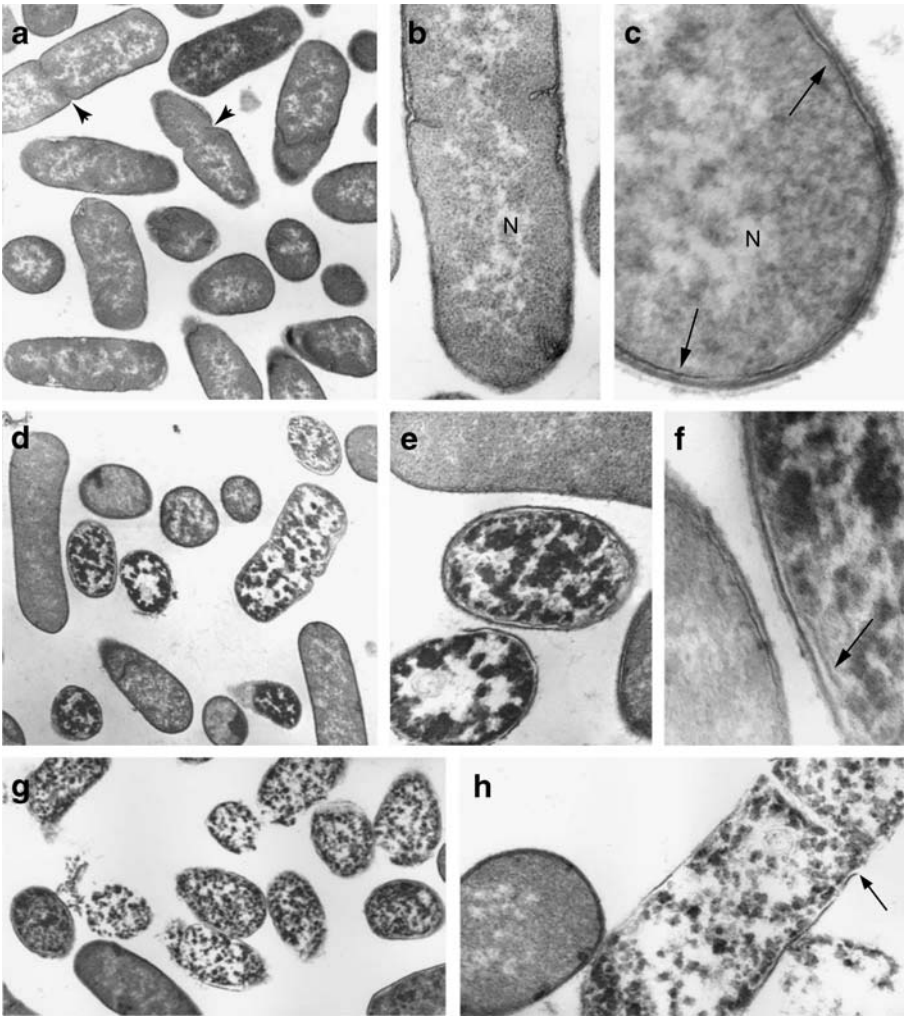

Fig. 3 Transmission electron micrographs of *Bacillus stearothermophilus* from cultures at the exponential phase (**a**–**c**), stationary phase (**d**–**f**), and stationary phase after treatment with methoprene (**g**, **h**). **a** Typical population of bacteria, some of which undergoing division (*arrowheads*); **b** detail of a cell at the beginning of division showing the scattered fibrillar nucleoid (*N*); **c** periphery of a cell showing the densely stained plasma membrane (*arrows*) and the overlying cell wall; **d** heterogeneous population of bacteria; **e** detail of bacteria with masses of dense material; **f** periphery of a normal and an abnormal bacteria, the latter showing a less stained plasma membrane (*arrow*); **g** population of disrupted bacteria after treatment with methoprene; **h** detail of a disrupted cell showing the breakage of the cell wall and the plasma membrane (*arrow*). Magnifications: ×15,000 (**a**, **d**, **g**), ×35,000 (**b**, **e**, **c**), ×100,000 (**c**, **f**)

collected at two different times: immediately before the addition of the insecticide (at the latter exponential phase, after 60 min of incubation) and 1 h after (at the stationary phase, after 120 min of incubation). Control cultures harvested 60 min after incubation showed a very uniform population of rod-shaped cells (Fig. 3a) in which the cytoplasm was finely granular with evenly distributed ribosomes (Fig. 3b). The nucleoid was usually represented by scattered electronlucent areas containing coarse fibrils (Fig. 3b,c). Figures of cell

Table 1 Percentage of cells examined with the TEM showing absence (normal) or presence of ultrastructural abnormalities (abnormal cells).

Samples (min)	Normal cells (%)[a]	Abnormal cells (%)[a]
Control 60 min	96.32±1.63 (10)	3.68±1.63 (10)***
Control 120 min	70.47±4.73 (12)	29.53±4.73 (12)***
Methoprene 120 min	46.44±8.20 (13)	53.56±8.20 (13)** §§§

Aliquots from cultures grown in the control conditions were harvested after 60 or 120 min of incubation (control 60 min or control 120 min) and aliquots from cultures at which 20 μM methoprene was added at the later exponential phase (after 60 min of incubation) were harvested 1 h after the insecticide addition (methoprene 120 min).

[a] Values of cell counts are means ± standard deviation from 10 or more (*number in brackets*) count areas, and comparisons were performed using one-way ANOVA, with the Student–Newman–Keuls as a post-test, for the following paired observations: abnormal cells vs normal cells from the same sample (control 60 min, control 120 min, or methoprene 120 min), ***$p<0.001$ and **$p<0.01$; abnormal cells from the methoprene 120-min sample vs abnormal cells from control 120 min sample, *$p<0.001$.

division were frequently seen, this being initiated at a cellular medial position by the formation of a septal cross wall (Fig. 3a,b). At higher magnification, the cell wall consisted of an outermost layer (S layer) that was fibrilar, weakly electrondense, and most of the times poorly defined, and a next inner layer (peptidoglycan-containg layer) that was homogeneously electrondense and compact and separated from the plasma membrane by a relatively thin electronlucent space (Fig. 3c). The plasma membrane appeared always deeply stained after the fixation technique used, showing the typical asymmetric geometry (Fig. 3c). A few plasma membrane invaginations were sometimes seen. Control cultures harvested 120 min after incubation showed a reasonably more heterogeneous cell population (Fig. 3d) than those previously referred. A higher percentage of damaged or morphologically abnormal cells was noticed (Fig. 3d and Table 1). These cells showed evident signals of disorganization, being characterized by numerous dense masses of amorphous material resulting from the cytoplasmic matrix coagulation (Fig. 3d–f). Neither ribosomes nor the typical nucleoid areas were evident in these cells. Also, division of the cells was only seen sporadically. In the damaged cells, the plasma membrane is usually less electrondense than in the normal cells showing a symmetric profile (Fig. 3f). The cell wall either remained apparently unchanged or was damaged locally, and consequently, some cells were seen disrupted (Fig. 3e). Cultures treated with methoprene clearly showed the highest percentage of damaged cells (Fig. 3g and Table 1). These cells showed characteristics identical to those of the 120-min control cultures (cf. Fig. 3d with Fig. 3g). However, a higher number of disrupted cells were clearly produced as a result of breakage of both the cell wall and the plasma membrane (Fig. 3h).

Methoprene Effects on the Physical State of Lipid Bilayers

The effects of methoprene on the physical properties of the lipid bilayer were studied in membrane models of DMPC and DPPC and in lipid dispersions prepared with the polar lipid fraction or the total lipid extract of *B. stearothermophilus* grown at 65 °C. The total lipid extract of the bacterium consists of neutral lipids, including carothenoids, and polar lipids (PL) represented by phospholipids (phosphatidylethanolamine, which corresponds to 80% of the total lipid phosphorus content, cardiolipin, and phosphatidylglycerol) and a phosphoglycolipid [13].

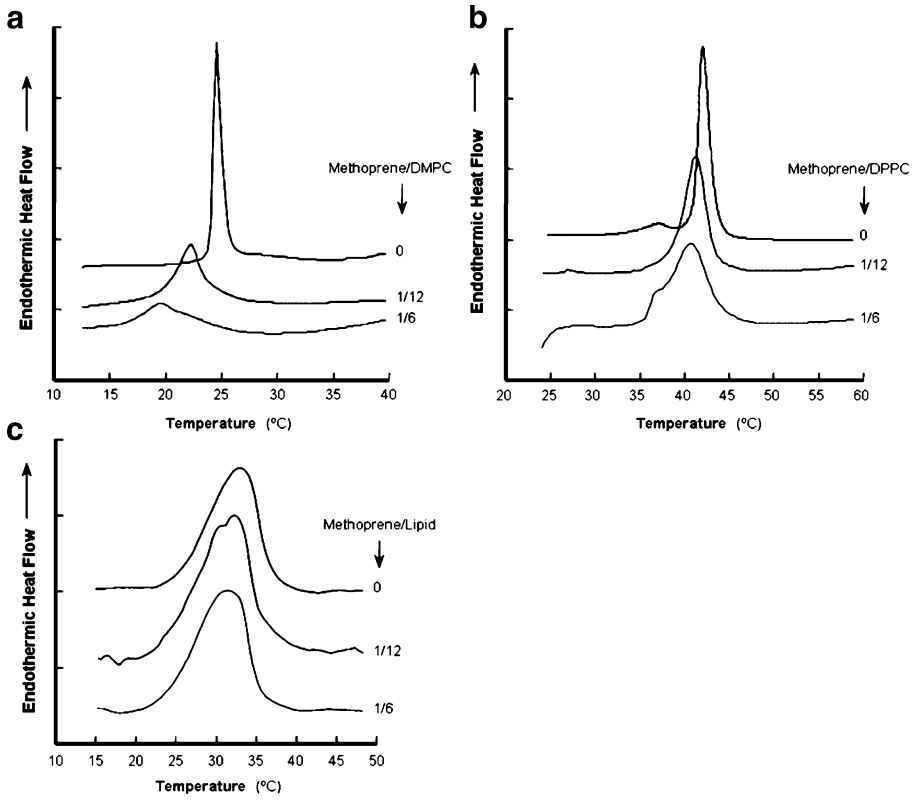

Fig. 4 Effects of methoprene on DSC thermograms of DMPC (**a**), DPPC (**b**), and the total lipid extract of *B. stearothermophilus* (**c**). The insecticide/lipid molar ratios are indicated on the scans. The DSC profiles are heating scans. The thermograms are typical assays of at least three independent experiments

Whereas the DSC scans of DMPC and DPPC bilayers showed a sharp transition peak, the bacterial lipids (total lipid extract) dispersions displayed a broad endotherm spanning over a range of about 15 °C (Fig. 4). The thermotropic profile (heat scan) of multilamellar vesicles of DPPC also showed a pre-transition at 36.2 °C, preceding the main transition at 42.7 °C (Fig. 4, Table 2).

The incubation of DMPC or DPPC bilayers with the insecticide (30 to 60 μM) promoted a shift of the temperature at which lipid dispersions, when heated, undergo a gel to liquid-crystalline phase transition (T_m). Bacterial lipids dispersions prepared with the heterogeneous mixture of lipids extracted from *B. stearothermophilus* were also affected by methoprene. The latter induced a shift of the temperature at which the transition is 50% complete (T_m). In all lipid preparations, the T_m shifted toward lower temperatures, and the T_m shift showed to be dependent upon the insecticide/lipid ratio (Fig. 4, Table 2). A T_m shift of about 2.5 to 3.0 °C was observed with the highest insecticide/lipid molar ratio assayed. Also, methoprene induced a shift toward lower temperatures of the onset (T_o) and completion (T_f) of both the DMPC and DPPC phase transitions and the bacterial lipids lateral phase separation (Fig. 4).

The bilayers prepared with the pure synthetic lipids (DMPC and DPPC) showed a significant broadening in the presence of the insecticide (Fig. 4 and Table 2). In the case of DPPC vesicles, methoprene abolished the pre-transition peak (Fig. 4). In these vesicles, a

Table 2 Characterization of the phase transitions detected by DSC (temperature of the endothermic peak, T_m, transition temperature range, $T_f - T_o$, and enthalpy change, ΔH) or fluorescence polarization of DPH and DPH–PA (temperature of the peak of derivative curves, T_m') in liposomes prepared with the synthetic lipids DMPC or DPPC and with the total lipids (TL) or the polar lipids (PL) extracted from cells of *B. stearothermophilus*.

Liposome lipid composition	*Methoprene* Lipid molar ratio	Fluorescence polarization T_m' (°C)		DSC T_m (°C)	$T_f - T_0$ (°C)	ΔH (J/g)
		DPH	DPH–PA			
DMPC	0	25.00±0.19	24.79±0.36	24.42±0.21	2.34±0.35	21.63±2.24
	1/12	23.10±0.32, n.s.	22.05±0.17*	23.03±0.12**	4.69±0.20**	21.92±2.03 n.s.
	1/6	22.91±0.50*	19.99±0.31*	21.85±0.46***	7.07±0.32**	21.95±2.55, n.s.
DPPC	0	42.78±0.17	42.86±0.23	42.65±0.18	2.95±0.24	37.43±3.30
	1/12	40.67±0.33*	41.61±0.14***	40.68±0.15*	5.49±0.48*	38.07±3.51, n.s.
	1/6	39.80±0.14***	40.44±0.07**	39.92±0.05***	7.38±0.42**	39.37±4.02, n.s.
TL (or PL)	0	32.41±0.19	33.07±0.29	32.68±0.09	12.33±0.40	17.83±1.79
	1/12	31.30±0.18**	32.17±0.30*	30.78±0.32, n.s.	12.45±0.34*	18.23±2.08, n.s.
	1/6	30.88±0.16***	31.16±0.19**	29.60±0.12*	13.08±0.45*	18.20±1.90, n.s.

Liposomes were incubated with methoprene to obtain insecticide/lipid molar ratios of 1:12 and 1:6 or with a few microliters of ethanol (corresponding to the maximal volume of the methoprene solution assayed) for the control (methoprene/lipid molar ratio of zero in the table). Values presented are means ± standard deviation of 3 fluorescence polarization experiments or four DSC experiments. Comparisons were performed using one-way ANOVA, with the Student–Newman–Keuls as a post-test for the following paired observations: liposomes with a methoprene/lipid ratio of 1:12 or 1:6 vs control liposomes (without methoprene).

n.s. Not significant

*$p<0.05$

**$p<0.01$

***$p<0.001$

small shoulder toward lower temperatures on the main transition peak was noticed after incubation with the highest methoprene concentration (60 μM, corresponding to an insecticide/lipid molar ratio of 1:6). This may indicate a tendency to create a lateral heterogeneity in the membrane, with the lipid domains enriched in the insecticide, showing a phase transition at lower temperatures than that of the rest of the bilayer. This heterogeneity may explain the decrease of the cooperative transition reflected by the broadening of the endotherm. Although this effect could also occur in the bilayers prepared with the mixture of the bacterial lipids, it may be not apparent as a result of the heterogeneous lipid composition of the liposomes undergoing a lateral phase separation instead of a phase lipid transition.

Important quantitative information provided by the thermotropic transition profiles concerns the enthalpy of the transition that reflects the hydrophobic interactions in the acyl chains of the phospholipids. This thermodynamic parameter is quantitatively lower as the acyl chain shortens, being consistently higher for DPPC than for DMPC bilayers (Table 2). The lowest value was registered in the bacterial lipid dispersions (Table 2) because of the heterogeneous acyl chain composition and the different polar groups of the phospholipids, which contribute to a lower packing of the lipid bilayer. Methoprene seems not to significantly affect the enthalpy change of the transition from the gel to the liquid-crystalline phase of DMPC and DPPC membranes, as well as the enthalpy change of the bacterial lipids lateral phase separation.

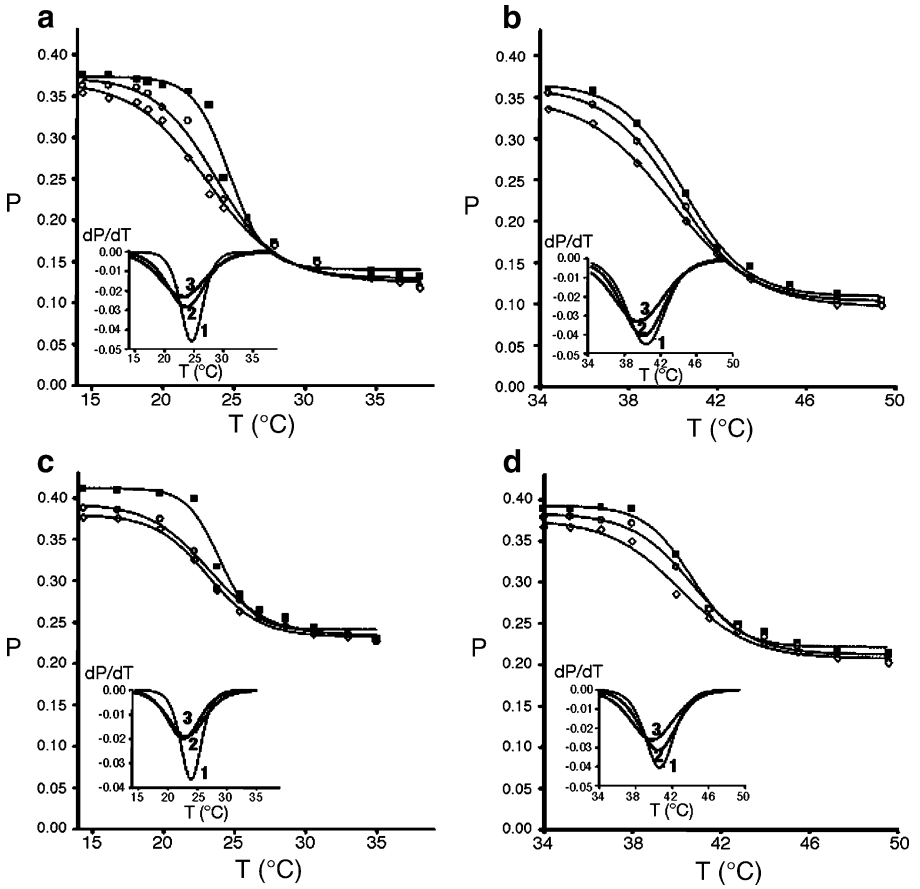

Fig. 5 Thermograms of fluorescence polarization (*P*) of DPH (**a** and **b**) and DPH–PA (**c** and **d**) in liposomes prepared with DMPC (**a** and **c**) or DPPC (**b** and **d**). Liposomes were incubated with 30 μM methoprene (*circle*), 60 μM methoprene (*diamond*), or with a few *microliters* of ethanol, corresponding to the maximal volume of the methoprene solution assayed (*square*). The derivative curves *1*, *2*, and *3* (*inset*) correspond to the main curves with the symbols *square*, *circle*, and *diamond*, respectively. The thermotropic profiles are typical assays of at least three independent experiments, and the polarization values are means of three readings of fluorescence intensities for each temperature. The standard deviations are too small to be displayed by error bars, as, for most points, they are encompassed by the size of the *symbols*

Concerning the thermograms of fluorescence polarization, the fluidity-related spectroscopic parameter (*P*) in the DMPC and DPPC bilayers undergoes, as expected, an abrupt decrease with the temperature increase, thus, reflecting a sharp phase transition (Fig. 5). A more smooth decrease is observed in the bacterial polar lipid dispersions (Fig. 6). The latter differ from those used for DSC scans by the fact that the neutral lipids were excluded from the lipid extract. Derivative curves determined by a computer graph program (insets in Figs. 5 and 6) allow us to recognize the temperature range of the transition phase (approximately 3 °C for the synthetic lipid bilayers and 15 °C for the bacterial polar lipid dispersions), as well as the transition temperature midpoint (T_m) that corresponds to the peak of the fluorescence polarization derivative curve. The T_m values detected by means of the fluorescent probes and those provided by the DSC traces (Table 2) show a reasonable accordance in all membrane preparations, including those of bacterial lipid extracts that

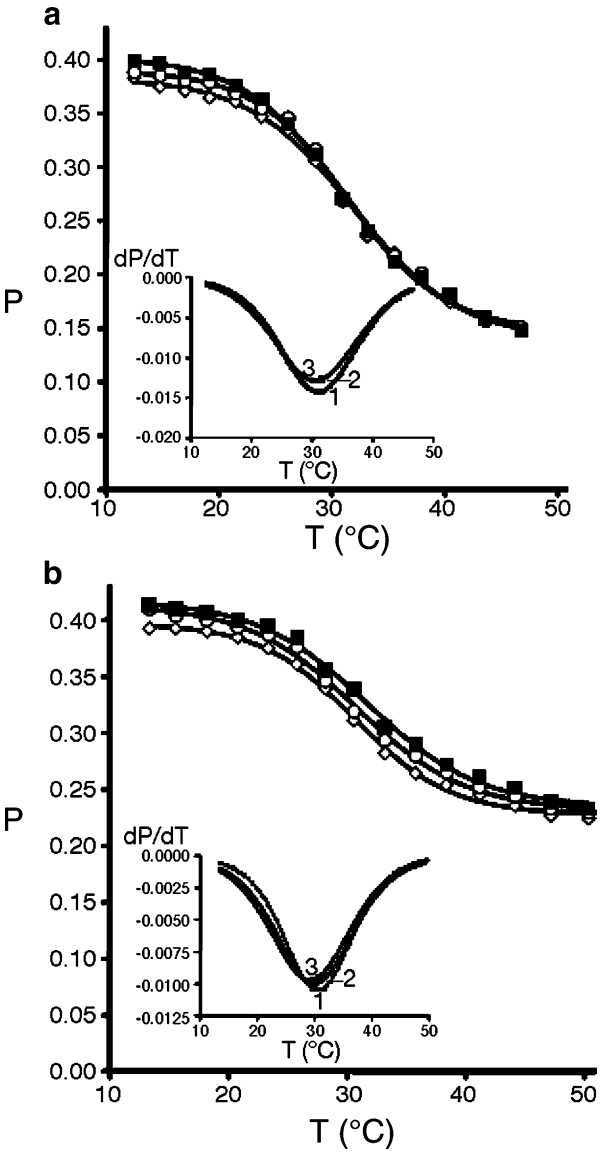

Fig. 6 Thermograms of fluorescence polarization (*P*) of DPH (**a**) and DPH–PA (**b**) in liposomes prepared with the polar lipid extract of *B. stearothermophilus*. Liposomes were incubated with 30 μM methoprene (*circle*), 60 μM methoprene (*diamond*), or with a few *microliters* of ethanol, corresponding to the maximal volume of the methoprene solution assayed (*square*). The derivative curves *1*, *2*, and *3* (*inset*) correspond to the main curves with the symbols *square*, *circle*, and *diamond*, respectively. The thermotropic profiles are typical assays of at least three independent experiments, and the polarization values are means of three readings of fluorescence intensities for each temperature. The standard deviations are too small to be displayed by error bars, as, for most points, they are encompassed by the size of the *symbols*

differ in the neutral lipid content. This suggests that the bacterial polar lipids (representing 80–90%, by weight, of the total lipid extract) (13) are the main lipids responsible for the thermotropic behavior of the bacterial membrane lipid bilayers.

Fluorescence polarization was performed using two probes located in different regions across the bilayer thickness: DPH, buried in the hydrocarbon core [25], and DPH-PA anchored close to the bilayer surface because of its charged group [26]. The fluorescence polarization reported by the two probes in the respective environments, at the same temperature, reflects an increase of fluidity from the outer regions toward the core of the bilayer (Figs. 5 and 6), in agreement with classical reports [27].

Consistent with DSC data, the fluorescence polarization thermograms of DPH and DPH–PA incorporated in liposomes of the synthetic lipids DMPC and DPPC show that the addition of methoprene (30 to 60 μM) lowers the phase transition temperature and broadens the transition profile, affecting cooperativity (Fig. 5 and Table 2). With increasing concentrations of insecticide, the above membrane preparations exhibited, as compared to the control, a decrease of fluorescence polarization of DPH and DPH-PA in the gel phase and in the transition temperature range. This reflects a decrease of the structural order of the lipid membranes across the bilayer thickness. In bacterial lipid dispersions, methoprene also induced a decrease of the structural order (Fig. 6). However, its action at different depths of the bilayer depends on the lipid phase. Thus, below the lateral phase separation, methoprene perturbs the lipid order across the bilayer thickness. In the transition temperature range and at higher temperatures, methoprene does not affect the center of the bilayer, its action being restricted to the outer regions of the lipid membranes monitored by DPH–PA.

Discussion

The present study is included in a larger project aimed to correlate the effects of pesticides on membrane lipid organization with deleterious alterations at the cell/organism level. As the structure and dynamics of the lipid bilayer are critical for most membrane activities, including permeability [10], xenobiotic-induced disordering and disturbance of the membrane stability may compromise cell function and viability. Considering that many vital cell functions are ascribed to the bacterial plasma membrane [28, 29], prokaryotic cells are particularly useful to assess cytotoxicity of membrane-active drugs on the basis of perturbations of cell growth and viability. The eubacterium *B. stearothermophilus* has revealed high sensitivity to adverse agents affecting the physical state of membrane lipids, as has been extensively studied by our group for a variety of lipophilic drugs and pollutants [15, 16, 30–32]. We previously showed [16] that methoprene promotes growth impairment and loss of viability of *B. stearothermophilus* cells when added to the culture medium in the beginning of growth. These effects are reverted by the presence of Ca^{2+}, a membrane stabilizer [13, 33]. Furthermore, we showed that methoprene inhibits the respiratory activity of bacterial protoplasts [16]. In the present work, the decrease of bacterial yield (Fig. 2) and the cell ultrastructural alterations prematurely induced in the retardation phase, including cell lysis (Fig. 3), is evidence of the cytotoxic effects caused by methoprene added to the cultures in the exponential phase.

As many other pesticides [34], methoprene has a high lipophilic character [9] in consequence of which a strong interaction with membrane lipids is predictable. The biophysical studies performed by means of fluorescence polarization and DSC provided different experimental approaches. DSC data provided information about the transition temperature and the enthalpy change. Fluorescent probes allowed us to further characterize the thermotropic behavior of lipids, monitoring the structural order below and above the phase transition or the lateral phase separation temperature range. In addition, the total lipid extract of the bacterial membranes was studied by DSC but not by spectrofluorimetry because the presence of fluorescent neutral lipid components induced a significant fluorescence quenching of fluidity probes. The overall effects of the increasing concentrations of methoprene on the thermotropic behavior of DMPC, DPPC, and bacterial lipid extracts are compatible, according to Jain and Wu [35], with the methoprene molecule aligning itself with the prevailing direction of the phospholipid acyl chains, disrupting their

packing, reducing the co-operativity of the transition, and shifting the phase transition temperatures to lower values.

It is worth noting that the membrane physical effects, denoted in bacterial lipid membranes by a perturbation across the bilayer thickness (Fig. 6) and the induction of cell structural changes (Fig. 3) occur at similar concentration ranges of methoprene, which suggests that these events are correlated, concurring to the toxicity of the insecticide. Altogether, the above referred studies indicate that the methoprene-induced adverse effects on bacterial cells are most likely mediated by insecticide–membrane lipids interactions.

In conclusion, by revealing the membrane activity of methoprene, the present data provide novel insights to the understanding of the molecular mechanisms underlying non-selective effects of this insecticide on non-target organisms.

References

1. Corbett, J. R., Wright, K., & Baillie, A. C. (1984). *The biochemical mode of action of pesticides* (pp. 224–225). London: Academic.
2. Breaud, T. P., Farlow, J. E., Steelman, C. D., & Schilling, P. E. (1977). *Mosquito News*, *37*, 704–712.
3. Templeton, N. S., & Laufer, H. (1983). *International Journal of Invertebrate Reproduction*, *6*, 99–110.
4. Quistad, G. B., Schooley, D. A., Staiger, L. E., Bergot, B. J., Sleight, B. H., & Macek, K. J. (1976). *Pesticide Biochemistry and Physiology*, *6*, 523–529.
5. McKague, A. B., & Pridmore, R. B. (1978). *Bulletin of Environmental Contamination and Toxicology*, *20*, 167–169.
6. La Clair, J. J., Bantle, J. A., & Dumont, J. (1998). *Environmental Science & Technology*, *32*, 1453–1461.
7. Stocum, D. L. (2000). *Teratology*, *62*, 147–150.
8. Ankley, G. T., Degitz, S. J., Diamond, S. A., & Tietge, J. E. (2004). *Ecotoxicology and Environmental Safety*, *58*, 7–16.
9. Walker, A. N., Bush, P., Puritz, J., Wilson, T., Chang, E. S., Miller, T., et al. (2005). *Integrative and Comparative Biology*, *45*, 118–126.
10. Mouritsen, O. G., & Jorgensen, K. (1998). *Pharmaceutical Research*, *15*, 1507–1519.
11. Mouritsen, O. G. (2005). *Life as a matter of fat, the emerging science of lipidomics* pp. 159–172. Berlin: Springer-Verlag.
12. Jurado, A. S., Santana, A. C., Costa, M. S., & Madeira, V. M. C. (1987). *Journal of General Microbiology*, *133*, 507–513.
13. Jurado, A. S., Pinheiro, T. J. T., & Madeira, V. M. C. (1991). *Archives of Biochemistry and Biophysics*, *289*, 167–179.
14. Luxo, C., Jurado, A. S., & Madeira, V. M. C. (1998). *Biochimica et Biophysica Acta*, *1369*, 71–84.
15. Rosa, S. M. L. J., Antunes-Madeira, M. C., Matos, M. J., Jurado, A. S., & Madeira, V. M. C. (2000). *Biochimica et Biophysica acta*, *1487*, 286–295.
16. Monteiro, J. P., Jurado, A. S., Moreno, A. J. M., & Madeira, V. M. C. (2005). *Toxicology In Vitro*, *19*, 951–956.
17. Spurr, A. R. (1969). *Journal of Ultrastructure Research*, *26*, 31–43.
18. Bligh, E. G., & Dyer, W. J. (1959). *Canadian Journal of Biochemistry and Physiology*, *37*, 911–917.
19. Bartlett, G. R. (1959). *Journal of Biological Chemistry*, *234*, 466–468.
20. Bottcher, C. J. F., van Gent, C. M., & Pries, C. (1961). *Analytica Chimica Acta*, *24*, 203–204.
21. Antunes-Madeira, M. C., & Madeira, V. M. C. (1989). *Pesticide Science*, *26*, 167–179.
22. Donato, M. M., Antunes-Madeira, M. C., Jurado, A. S., & Madeira, V. M. C. (1997). *Bulletin of Environmental Contamination and Toxicology*, *59*, 696–701.
23. Shinitzky, M., & Barenholz, Y. (1978). *Biochimica et Biophysica Acta*, *515*, 367–394.
24. Lentz, B. R. (1989). *Chemistry and Physics of Lipids*, *50*, 171–190.
25. Andrich, M. P., & Vanderkooi, J. M. (1976). *Biochemistry*, *15*, 1257–1261.
26. Trotter, P. J., & Storch, J. (1989). *Biochimica et Biophysica Acta*, *982*, 131–139.
27. Tilley, L., Thulborn, K. R., & Sawyer, W. H. (1979). *Journal of Biological Chemistry*, *254*, 2592–2594.
28. Stock, J. B., Stock, A. M., & Mottonen, J. M. (1990). *Nature*, *344*, 395–400.
29. Trumpower, B. L., & Gennis, R. B. (1994). *Annual Review of Biochemistry*, *63*, 675–716.

30. Donato, M. M., Jurado, A. S., Antunes-Madeira, M. C., & Madeira, V. M. C. (2000). *Archives of Environmental Contamination and Toxicology*, *39*, 145–153.
31. Martins, J. D., Monteiro, J. P., Antunes-Madeira, M. C., Jurado, A. S., & Madeira, V. M. C. (2003). *Toxicology In Vitro*, *17*, 595–601.
32. Monteiro, J. P., Martins, J. D., Luxo, P. C., Jurado, A. S., & Madeira, V. M. C. (2003). *Toxicology In Vitro*, *17*, 629–634.
33. Mosley, G. A., Card, G. L., & Koostra, W. L. (1976). *Canadian Journal of Microbiology*, *22*, 468–474.
34. Ecobichon, D. J. (2003). Toxic effects of pesticides. In C. D. Klaassen, & J. B. Watkins (Eds.), *Casarett & Doull's essentials of toxicology* (pp. 333–347). New York: McGraw-Hill.
35. Jain, M. K., & Wu, N. M. (1977). *Journal of Membrane Biology*, *34*, 157–201.